Journal of Catalysis **209,** 87–98 (2002)
doi:10.1006/jcat.2002.3623

Acetic Acid Reduction by H_2 on Bimetallic Pt–Fe Catalysts

Willy Rachmady and M. Albert Vannice[1]

Department of Chemical Engineering, Pennsylvania State University, University Park, Pennsylvania 16802-4400

Received November 5, 2001; revised March 29, 2002; accepted April 1, 2002

Vapor-phase acetic acid hydrogenation was studied over a family of supported Pt–Fe catalysts. These catalysts were characterized by Mössbauer spectroscopy, successive H_2–O_2–H_2–O_2 titration cycles at 300 K, and DRIFTS (diffuse reflectance FTIR spectroscopy) to determine the Fe phases present during the titration reactions as well as prior to and under reaction conditions, to count surface metal atoms and estimate the average surface composition of the bimetallic particles, and to observe surface species formed after acetic acid adsorption, respectively. Although the metallic mole fraction of Pt in the bimetallic Pt–Fe/SiO_2 catalysts varied from 0.04 to 0.64, the estimated surface composition in the bimetallic particles ranged from 0.39 to 0.70. The addition of small amounts of Pt to Fe/SiO_2 catalysts (i) increased Fe reducibility during the reduction pretreatment, (ii) enhanced activity more than 10-fold and turnover frequencies 10- to 100-fold, (iii) eliminated the induction period, (iv) lowered the apparent activation energy by 8–10 kcal/mol, and (v) still maintained a high selectivity to acetaldehyde of over 70%. The addition of Pt to an Fe/C catalyst prevented the severe deactivation that has been associated with iron carbide formation. Under reaction conditions, the best bimetallic catalyst contained both Fe^0 and Fe^{2+} phases, which is a combination that seems to be required for stable selective acetaldehyde formation. A model consistent with our previous studies of Pt and Fe catalysts, which invokes one type of active site on a reduced metal surface and another type on a metal oxide phase, successfully describes this reaction on a bimetallic catalyst. It is proposed that the reaction sequence involves a rate-determining step between a hydrogen atom from the metallic site and an acyl species on the FeO surface. © 2002 Elsevier Science (USA)

INTRODUCTION

Recent studies in our laboratory have provided strong evidence that the catalytic chemistry associated with acetic acid reduction by H_2 over Pt or Fe is governed by the presence of both metal and metal oxide phases present under reaction conditions (1, 2). The kinetics of this reaction on Pt/TiO_2 and Fe/SiO_2 were consistent with a mechanism requiring sites on the zero-valent metal to activate H_2 and different sites on an oxide phase to activate acetic acid; regardless, different catalytic behavior was observed between these Pt and Fe catalysts. For example, titania-supported Pt was a very active reduction catalyst which yielded mainly ethanol, ethane, and ethyl acetate, whereas silica-supported Fe was highly selective for acetaldehyde formation although much higher temperatures were required for significant activity to be achieved. In an effort to develop more active yet highly selective catalysts for the reduction of carboxylic acids to aldehydes, bimetallic Pt–Fe systems were investigated to determine if the most favorable characteristics exhibited by each metal could be combined in a single catalyst.

Bimetallic Pt–Fe catalysts have been used in various applications such as CO hydrogenation (3–5), catalytic combustion in automotive catalysts (6), and cathodic oxygen reduction in fuel cells (7, 8). In most cases, iron was added to a Pt catalyst to enhance activity and control selectivity, as demonstrated by the increase in oxygenate selectivity during CO hydrogenation over a Pt–Fe catalyst as compared to Pt alone (5). In the case of cathodic oxygen reduction, Pt–Fe catalysts generally show a greater activity, although the precise reason for the enhancement is still being debated because of uncertainty associated with the specific activity measurements (7). In automotive exhaust catalysts, Fe was added to a Pt catalyst to improve its thermal stability because the presence of Fe appeared to prevent Pt sintering (6, 9).

In the present study, catalysts were impregnated with both Pt and Fe to increase activity and improve selectivity to acetaldehyde during acetic acid hydrogenation by utilizing the favorable properties of each metal. In accordance with the apparent dual site nature of the proposed catalytic cycle, metallic Pt and Fe atoms were expected to provide sites for hydrogen adsorption and dissociation while iron oxide phases would provide sites to adsorb and activate acetic acid in a manner to maximize acetaldehyde formation. These two types of sites are presumed to be in contact for the reaction to occur unless one active surface species, such as spilled-over H atoms, is capable of migrating significant distances. Characterizing the surface of bimetallic systems has always been a challenge, not only because surface and bulk stoichiometries can frequently differ following a given reduction pretreatment (3), but also because bimetallic clusters of different size and composition can exist; thus, an accurate interpretation of their catalytic behavior is

[1] To whom correspondence should be addressed. E-mail: mavche@engr.psu.edu.

0021-9517/02 $35.00
© 2002 Elsevier Science (USA)
All rights reserved.

TABLE 1

H_2 and O_2 Uptakes during Successive H_2–O_2–H_2–O_2 Titration Cycles on a Series of Pt–Fe Catalysts

Catalyst[a]	Analyzed loading (wt%)		Irreversible H_2 and O_2 uptakes (μmol/gcat)				Irreversible $H_2 : O_2 : H_2 : O_2$ ratios
	Pt	Fe	1st H_2 (Step 1)	1st O_2 (Step 2)	2nd H_2 (Step 3)	2nd O_2 (Step 4)	
0.7Pt/SiO_2	0.69	0	—	6.8[b]	—	—	—
0.7Pt/SiO_2	0.69	0	8.9 (14.6)[b,c]	—	—	—	—
0.7Pt/SiO_2	0.69	0	8.9 (14.6)[c]	11.2	23.6	11.6	1 : 1.3 : 2.6 : 1.3
0.7Pt–0.1Fe/SiO_2	0.69	0.11	9.7 (16)	20.1	37.0	18.0	1 : 2.1 : 3.8 : 1.9
0.7Pt–0.2Fe/SiO_2	0.69	0.23	8.3 (13.8)	23.5	28.0	14.0	1 : 2.8 : 3.4 : 1.7
0.7Pt–1Fe/SiO_2	0.67	1.0	8.6 (13.3)	54.5	28.0	13.9	1 : 6.3 : 3.3 : 1.6
0.7Pt–5Fe/SiO_2	0.62	4.9	4.9 (9.1)	320	20.0	10	1 : 65 : 4.1 : 2.0
0.6Pt–5Fe/carbon	0.62	5.4	3.3 (9.3)	290	50.1	32.9	1 : 88 : 15 : 10
3Fe/SiO_2	0		0.6 (1.0)	64.9	0.4	0.5	1 : 108 : 0.7 : 0.8

[a] Nominal weight percent loadings.
[b] Measured separately.
[c] Number in parentheses denotes the total H_2 uptake (reversible + irreversible).

often difficult to attain. Bartholomew and Boudart utilized an approach consisting of O_2–H_2–O_2 titration cycles coupled with Mössbauer spectroscopy to estimate the surface composition of Pt–Fe catalysts (10); however, this method is limited to highly dispersed catalysts because as the metal particle size increases, the surface/volume ratio decreases and the contribution from the surface iron atoms to the Mössbauer spectrum cannot be determined accurately. In the present study, a slightly different version of this cyclic titration technique was developed in an effort to characterize the surfaces that exist in bimetallic Pt–Fe crystallites, and this technique was particularly useful in characterizing large, reduced Pt–Fe particles which were commonly obtained with the Fe/SiO_2 systems. To increase activity for selective acetic acid hydrogenation and to improve our understanding of the mechanistic details of this reaction, a family of SiO_2-supported Fe, Pt, and Pt–Fe catalysts was investigated. A kinetic model proposed previously (11) was successfully applied to describe the kinetics of acetic acid reduction with H_2.

EXPERIMENTAL

SiO_2-supported Pt–Fe catalysts were prepared via a sequential impregnation approach. The silica gel support (Davison, Grade 57, 70–120 mesh) was calcined at 773 K for 2 h under 100 cm^3 (STP)/min of air (MG Ind., 99.5%) to remove any organic contaminants before metal impregnation. Platinum was deposited onto the silica via an ion exchange method using $Pt(NH_3)_4(OH)_2$ (Aldrich, 99.995%) as the metal precursor (12), and the dispersion of this base 0.7% Pt/SiO_2 was 0.83, based on total H_2 adsorption, or 0.49, based on the irreversible hydrogen uptake (see Table 1). After drying in an oven overnight at 393 K in air, Fe was deposited via an incipient wetness technique using $Fe(NO_3)_3 \cdot 9H_2O$ (Aldrich, 99.995%) dissolved in distilled, deionized (DD) water (2.2 cm^3/g SiO_2), and the catalyst was again dried overnight at 393 K in air. A carbon-supported Pt–Fe catalyst was also prepared by sequentially impregnating carbon black with a solution of $Fe(NO_3)_3 \cdot 9H_2O$ (3.4 cm^3/g carbon), drying, then reimpregnating with a solution of $H_2PtCl_6 \cdot 6H_2O$ (Aldrich, 99.995%). The carbon support (Black Pearls 2000, Cabot Corp.) was desulfurized for 12 h at 1223 K under 200 cm^3 (STP)/min H_2 (99.999%, MG Ind.) prior to impregnation. The exact metal loadings, expressed in weight percent, were determined by atomic absorption spectroscopy, and they are listed in Table 1. For simplicity, the catalysts are identified by the nomenclature *a*Pt–*b*Fe/SiO_2 (or/carbon) where *a* is the nominal weight percent Pt and *b* is the nominal weight percent Fe.

Catalyst pretreatment involved reduction in flowing H_2 for 1 h at 723 K after heating at 3 K/min to this temperature and was carried out *in situ* to prevent exposure of the catalyst to air before its use in any experiment. Chemisorption experiments were carried out in a stainless steel adsorption system with a base pressure of 1×10^{-6} Torr in the sample cell (13). The kinetic behavior of vapor-phase acetic acid reduction by H_2 was studied using a glass microreactor operated under differential conversions at atmospheric pressure, as already described elsewhere (1). Mössbauer spectroscopy and diffuse reflectance infrared Fourier-transform spectroscopy (DRIFTS) were also used to further characterize the iron phases and the surface species; details regarding the experimental setup have been given elsewhere (14).

RESULTS AND DISCUSSION

H_2–O_2–H_2–O_2 Titration Cycles

A method involving successive H_2–O_2–H_2–O_2 titration cycles was developed to help characterize these supported bimetallic Pt–Fe particles. The titration procedure, in principle, is similar to a previous procedure utilized by

Bartholomew and Boudart (10), but the sequence of the H_2 and O_2 titrations applied here was modified according to the following description. First, hydrogen was adsorbed on a clean catalyst surface obtained by a high-temperature evacuation at 673 K for 1 h following the reduction pretreatment at 723 K. Second, the catalyst was exposed to O_2, which first titrated the irreversibly adsorbed hydrogen and then chemisorbed on the catalyst surface. Third, after evacuation, this catalyst surface was titrated with H_2 to produce H_2O and re-adsorb H atoms. Finally, this latter catalyst surface was retitrated with O_2. The H_2 and O_2 adsorption isotherms during these titration cycles were recorded at room temperature, with a 30-min evacuation period between the uptake measurements, and Table 1 lists the H_2 and O_2 uptakes during these successive H_2–O_2–H_2–O_2 titrations on a series of SiO_2-supported Pt–Fe catalysts and one carbon-supported Pt–Fe catalyst.

The chemisorption behavior of H_2 and O_2 on individual metallic Pt and Fe surfaces is largely understood. Both hydrogen and oxygen chemisorb atomically on a clean Pt surface, and one adsorbate can be completely titrated with the other at 300 K; consequently, the H_2 titration of chemisorbed oxygen on dispersed Pt has been frequently used to calculate the number of reduced Pt atoms (15, 16). Fe metal, on the other hand, does not exhibit the same H_2–O_2 titration behavior because H_2 chemisorption is typically negligible on reduced Fe surfaces at 300 K, at least on small dispersed Fe particles, whereas O_2 chemisorption can result in multilayer oxidation of Fe to subsurface levels that cannot be titrated by hydrogen at 300 K. However, it has been shown by Bartholomew and Boudart (10) as well as Garten (17) that oxidized Fe can be partially reduced by H_2 at 300 K when this Fe oxide phase exists in bimetallic particles, i.e., in direct contact with a noble metal such as Pt or Pd. Consequently, the reducibility of Fe oxide at 300 K is unique in that it is possible only when a noble metal capable of providing atomic hydrogen is in intimate contact with the iron phase.

Figure 1 displays Mössbauer spectra of the 0.7Pt–5Fe/SiO_2 catalyst obtained at 300 K following each adsorption step in the H_2–O_2–H_2–O_2 titration sequence. Spectrum Fig. 1a was recorded after the catalyst was reduced at 723 K and had chemisorbed hydrogen on its surface, and it shows that iron in the catalyst exists only as zero-valent Fe (α-Fe), as identified by the characteristic sextuplet of peaks for bulk metallic α-Fe. After titration with O_2, a part of the zero-valent iron was oxidized to Fe^{3+}, as shown by the appearance of a doublet in Fig. 1b having an isomer shift (IS) of 0.34 mm/s and a quadrupole splitting (QS) of 1.09 mm/s. A subsequent H_2 titration of this catalyst produced an additional doublet, having an IS of 0.99 mm/s and a QS of 1.83 mm/s, as indicated in Fig. 1c, which can be attributed to an Fe^{2+} phase. Finally, the last step in this sequence, i.e., O_2 titration, reoxidized the catalyst and left α-Fe and Fe^{3+} as the only iron phases detected in the catalyst, as shown by Fig. 1d, which is essentially the same as Fig. 1b. Based on these Mössbauer spectra, it can be seen that all the iron is completely reduced after the initial pretreatment in the presence of Pt, but following the first O_2 titration reaction, some of this iron is oxidized to Fe^{3+}(Fe_2O_3), a portion of which can be reduced to Fe^{2+} by H_2 at 300 K. The complete initial reduction of iron to Fe^0 and the partial reduction of Fe_2O_3 to FeO at 300 K is strong evidence that there was direct contact between Fe and Pt in bimetallic Pt–Fe particles dispersed on the support (3, 10, 17). The term bimetallic is used here to refer to any structure that provides direct physical contact between Pt and Fe atoms.

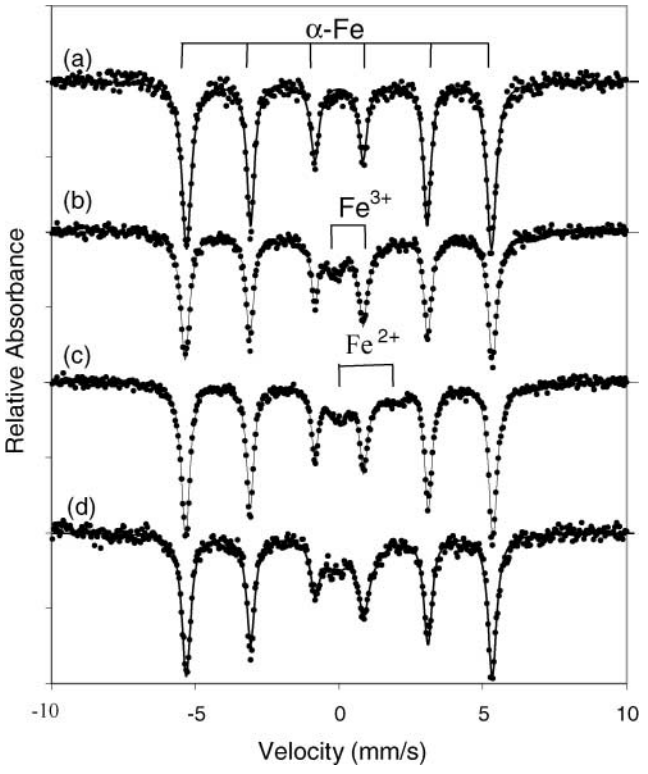

FIG. 1. Mössbauer spectra of 0.7Pt–5Fe/SiO_2 after (a) H_2 adsorption, (b) O_2 titration, (c) H_2 titration, and (d) O_2 titration. Spectral parameters are listed in Table 2.

More than a monolayer of chemisorbed oxygen was formed on the Fe surface during the first O_2 titration, and subsurface oxide layers were created. It has been reported that five to seven atomic layers of an iron oxide film can be formed as a result of oxidation by O_2 at room temperature (18–22), and this oxide layer cannot be reduced by hydrogen at room temperature unless it is in direct contact with Pt (3, 10). Thus the amount of Fe that is in direct contact with Pt, i.e., the Fe present in bimetallic crystallites, can be quantified by determining the amount of iron oxide that is reduced during hydrogen titration, but some assumptions must be made to accomplish this. The first one in the development of a model to describe the H_2–O_2–H_2–O_2 titration sequence is that the reduction of Fe_2O_3 to FeO is strictly a

surface phenomenon; consequently, although up to seven atomic layers of iron may have been oxidized during the first O_2 titration, only the top surface layer of any Fe_2O_3 in contact with Pt is assumed to be reducible by H_2 titration. The Mössbauer spectrum obtained following this H_2 titration (spectrum c in Fig. 1) shows that $Fe^{3+}(Fe_2O_3)$ was reduced to $Fe^{2+}(FeO)$, but further reduction to zero-valent Fe did not occur, in agreement with earlier studies using magnetic susceptibility measurements (23). The second assumption is that hydrogen does not irreversibly adsorb on oxidized iron surfaces. This assumption is substantiated by the fact that the ratio of irreversible (irr) uptakes of H_2 and O_2 measured for the last two cycles in the H_2–O_2–H_2–O_2 titration sequence remained constant as the Fe loading increased, i.e., there was no increase in the hydrogen uptake, relative to the subsequent O_2 uptake, despite an increase in the amount of iron oxide in the catalysts. Furthermore, no irreversible H_2 uptake was measured at 300 K on oxidized iron (2), and exposure of an oxidized Fe/Al_2O_3 catalyst to H_2 at 300 K produced no change in the Mössbauer spectrum (3). The third assumption, based on the earlier discussion, is that minimal or no H_2 chemisorption occurs on small dispersed zero-valent Fe particles at 300 K. These last two assumptions are also supported by the results in Table 1 for 3% Fe/SiO_2 as well as by results reported recently for other Fe/SiO_2 catalysts (2), because H_2 adsorption at 300 K should be similar to or lower than that at 373 K, as verified elsewhere (2).

The mechanistic details of the successive H_2–O_2–H_2–O_2 titrations in these bimetallic systems, therefore, can be depicted by the following scheme (following the initial pretreatment).

Step 1: H_2 adsorption.

$$y\mathrm{Fe} + x\mathrm{Pt_s} + \frac{x}{2}\mathrm{H_2} \rightarrow x\mathrm{Pt_s}\text{–}\mathrm{H} + y\mathrm{Fe}. \qquad [1]$$

Step 2: O_2 titration.

$$x\mathrm{Pt_s}\text{–}\mathrm{H} + y\mathrm{Fe} + \frac{1}{4}\left(\frac{5}{2}x + 3y\right)\mathrm{O_2} \rightarrow x\mathrm{Pt_s}\text{–}\mathrm{O_{3/4}} + \frac{y}{2}\mathrm{Fe_2O_3} + \frac{x}{2}\mathrm{H_2O}. \qquad [2]$$

Step 3: H_2 titration.

$$x\mathrm{Pt_s}\text{–}\mathrm{O_{3/4}} + f\frac{y}{2}\mathrm{Fe_2O_3} + \frac{1}{2}\left(\frac{5}{2}x + fy\right)\mathrm{H_2} \rightarrow x\mathrm{Pt_s}\text{–}\mathrm{H} + fy\mathrm{FeO} + \left(\frac{3}{4}x + \frac{fy}{2}\right)\mathrm{H_2O}. \qquad [3]$$

Step 4: O_2 titration.

$$x\mathrm{Pt_s}\text{–}\mathrm{H} + fy\mathrm{FeO} + \frac{1}{4}\left(\frac{5}{2}x + fy\right)\mathrm{O_2} \rightarrow x\mathrm{Pt_s}\text{–}\mathrm{O_{3/4}} + \frac{fy}{2}\mathrm{Fe_2O_3} + \frac{x}{2}\mathrm{H_2O}, \qquad [4]$$

TABLE 2

Mössbauer Spectral Parameters for 0.7Pt–5Fe/SiO_2 after Each Step in the H_2–O_2–H_2–O_2 Titration Cycle (as Shown in Fig. 1)[a]

Conditions	Phase	IS (mm/s)	QS (mm/s)	HF (kOe)	SC[b] (%)
H_2 adsorption (Step 1)	α-Fe	0.0	0.0	331	100
O_2 titration (Step 2)	α-Fe	0.0	0.0	332	75
	Fe^{3+}	0.34	1.09	—	25
H_2 titration (Step 3)	α-Fe	0.0	0.0	332	75
	Fe^{2+}	0.99	1.83	—	5
	Fe^{3+}	0.41	1.02	—	20
O_2 titration (Step 4)	α-Fe	0.0	0.0	331	78
	Fe^{3+}	0.41	1.10	—	22

[a] IS, isomer shift; QS, quadrupole splitting; HF, hyperfine field; and SC, spectral contribution.

[b] Uncertainty is ±5% of reported value.

where x is the number of surface Pt atoms, y is the number of Fe atoms oxidized during the first O_2 titration, and f is the fraction of Fe_2O_3 that is reducible to FeO, i.e., the surface Fe atoms in bimetallic particles. Then,

$$x = 2(\mathrm{H_2\ uptake\ in\ Step\ 1}), \qquad [5]$$

$$y = \frac{4(\mathrm{O_2\ uptake\ in\ Step\ 2}) - \frac{5}{2}x}{3}, \qquad [6]$$

and

$$f = \frac{2(\mathrm{H_2\ uptake\ in\ Step\ 3}) - \frac{5}{2}x}{y}. \qquad [7]$$

Independent measurements of H_2 and O_2 chemisorption on the $0.7Pt/SiO_2$ catalyst prior to the addition of Fe showed that the ratio of irreversible oxygen and hydrogen adsorption on Pt, i.e., the O_{ad}/H_{ad} ratio, is not unity but rather 3/4, as shown in Table 2; thus this stoichiometry was used in Eqs. [2] and [4]. This ratio of less than unity is not uncommon, particularly for highly dispersed Pt catalysts, and it is due to a change in the stoichiometry of oxygen chemisorption on $Pt(O_{ad}/Pt_s)$, which can vary from 1/2 on very small crystallites to near unity on large particles (24–26). Because all of the SiO_2-supported Pt–Fe catalysts underwent the same pretreatment as $0.7Pt/SiO_2$, it is assumed that this ratio of $O_{ad}/Pt_s = 3/4$ is the same for all of the catalysts and thus it is incorporated into the model. Although the coverage of irreversibly adsorbed H on very small Pt crystallites may be somewhat less than unity, a H_{ad}/Pt ratio of 1 is a good approximation and is used here for simplicity because H_{ad}/Pt ratios based on the total H_2 uptakes can be significantly greater than unity (24, 26–28). The important aspect is not that the H_{ad}/Pt ratio be precisely 1 but that this ratio remain constant.

The x, y, and f parameters can be calculated from the H_2 and O_2 uptakes measured during the titration cycles, as

depicted by Eqs. [5]–[7]. The number of surface Pt atoms is calculated using the irreversible H_2 uptake obtained during the first hydrogen adsorption in Step 1 and assuming an adsorption stoichiometry of unity, i.e., $2Pt_s + H_2 \rightarrow 2Pt_s$–H. This gives a minimum estimate of Pt_s because some weakly chemisorbed hydrogen can be desorbed during the 30-min evacuation between the two uptake measurements, and a full H monolayer may not exist (28, 29). Regardless of how the number of surface Pt atoms is determined, it is more important to know the ratio of irreversible oxygen and hydrogen chemisorption, which was experimentally found to be $O_{ad}/H_{ad} = 3/4$. Calculation of the overall Fe dispersion is not attempted here because the oxygen uptake by any monometallic Fe particles involves Fe oxidation up to several monolayers beneath the surface during the O_2 titration step. However, the total number of surface Fe atoms, Fe_s, will not be an appropriate parameter in determining the specific activity of these bimetallic Pt–Fe catalysts anyway because at lower temperatures monometallic Fe particles are essentially inactive; thus, the major contribution from Fe to the activity comes only from the surface Fe atoms in the bimetallic crystallites, referred to as $Fe_{s,bi}$, which can be calculated from the amount of FeO formed during the H_2 titration reaction depicted by Eq. [3] using the following relationship:

$$Fe_{s,bi}(\mu mol/gcat) = f \cdot y. \qquad [8]$$

To provide an example of these calculations, let us examine 0.7Pt–0.2Fe/SiO_2, for which 8.3 μmol/gcat H_2 irreversibly adsorbs on the catalyst during the first adsorption step. Based on this measurement, x, which is the minimum number of surface Pt atoms in the catalyst, is then 16.6 μmol Pt_s/gcat. During the first O_2 titration in Step 2, the O_2 uptake is 23.5 μmol/gcat, of which 4.2 μmol O_2/gcat is consumed to titrate the irreversibly adsorbed hydrogen on Pt, 6.2 μmol O_2/gcat is chemisorbed on the Pt, and the remaining 13.1 μmol O_2/gcat is consumed in the oxidation of Fe to Fe_2O_3, i.e., $2Fe + 3/2O_2 \rightarrow Fe_2O_3$; thus, the amount of Fe oxidized in this step (y) is 17.5 μmol/gcat. The last parameter to be calculated is f, the fraction of Fe_2O_3 that can be reduced during the H_2 titration reaction. Given that the irreversible H_2 uptake measured for 0.7Pt–0.2Fe/SiO_2 in Step 3 is 28.0 μmol H_2/gcat and is equal to $1/2(5/2x + fy)$, f is then 0.83; therefore, the concentration of surface bimetallic Fe atoms in 0.7Pt–0.2Fe/SiO_2, determined from Eq. [5], is $0.83(17.5) = 14.5$ μmol $Fe_{s,bi}$/gcat. A complete listing of the values calculated for the other catalysts is given in Table 3.

Reasonable values were obtained for the fraction of ferric oxide reducible to FeO, denoted as f(FeO) in Table 3, except for 0.7Pt–0.1Fe/SiO_2. Clearly this f value of 2.4 for 0.7Pt–0.1Fe/SiO_2 is meaningless because it cannot be greater than 1, and it indicates that the titration model developed above does not adequately describe the titration behavior of this catalyst. Aside from the fact that 0.7Pt–0.1Fe/SiO_2 was the only catalyst having more Pt than Fe, with a Pt/Fe ratio of 1.8, this catalyst also exhibited a H_2 uptake that was much higher than that needed to convert all the Fe_2O_3 into FeO, as depicted in Step 3. Two possible explanations can be proposed to account for this unexpectedly high H_2 uptake. First, there may have been a possible increase in H_2 uptake following the first O_2 titration step (Step 2) because the addition and oxidation of iron may have increased the dispersion of Pt. However, a second explanation is preferred; that is, ferric oxide may be reduced beyond FeO to a substoichiometric iron oxide (FeO_{1-x}) or even to zero-valent atoms during this H_2 titration. This extent of iron reducibility is possible and has been observed, particularly with Pt–Fe alloys containing a low Fe content. A Mössbauer study of a series of carbon-supported Pt–Fe catalysts showed that the appearance of the Fe^{2+} doublet in the spectrum following hydrogen titration became less pronounced as the iron content of the alloy was decreased (10), and a similar study of Pt–Fe/SiO_2 catalysts showed that Fe^{3+} in the samples having Pt/Fe ratios >1 was essentially reduced to zero-valent iron by H_2 titration (30). As pointed

TABLE 3

Concentration of Surface Pt and Fe Atoms in Pt–Fe Bimetallic Crystallites Estimated from H_2–O_2–H_2–O_2 Titration Cycles

Catalyst	Fe_t (μmol/gcat)	x^a (μmol/gcat)	y^b (μmol/gcat)	f(FeO)^c	f'(Fe)^d	Upper estimate $Fe_{s,bi}$ (μmol/gcat)	Lower estimate $Fe_{s,bi}$ (μmol/gcat)
0.7Pt–0.1Fe/SiO_2	19.7	19.4	10.6	2.4	0.80	25.4	8.5
0.7Pt–0.2Fe/SiO_2	41.2	16.6	17.5	0.83	0.28	14.5	4.8
0.7Pt–1Fe/SiO_2	179	17.2	58.3	0.22	0.074	13.0	4.3
0.7Pt–5Fe/SiO_2	877	9.8	419	0.037	0.012	15.5	5.2
0.6Pt–5Fe/carbon	970	6.6	381	0.22	0.073	83.7	27.9

[a] $x = Pt_s$ atoms.
[b] y = Fe atoms oxidized.
[c] f(FeO) = fraction of Fe^{3+} reducible to Fe^{2+} in bimetallic particles.
[d] f(Fe) = fraction of Fe^{3+} reduced to Fe^0 assuming this occurs.

out by Garten in a study of Pd–Fe catalysts, oxidized iron atoms with only Pd nearest neighbors, a situation obtained at high Pd/Fe ratios, can be completely reduced at 298 K (17). Therefore, iron atoms in the $0.7Pt–0.1Fe/SiO_2$ catalyst that have only Pt nearest neighbors may be reduced to the zero-valent state, which would result in the f value for this catalyst being grossly overestimated.

To consider the possibility that there are iron atoms in the catalysts having only Pt nearest neighbors, even when the overall Pt/Fe ratio is less than one, it is necessary to calculate another set of f values based on the assumption that ferric oxide in Pt–Fe clusters is reducible to the zero-valent state, and these are denoted as f(Fe) in Table 3. These values then give the minimum number of $Fe_{s,bi}$ atoms in the bimetallic clusters, and the titration in Step 3 is modified to

$$x\mathrm{Pt_s}\text{–}\mathrm{O}_{3/4} + f\frac{y}{2}\mathrm{Fe_2O_3} + \frac{1}{2}\left(\frac{5}{2}x + 3fy\right)\mathrm{H_2} \rightarrow x\mathrm{Pt_s}\text{–H} + fy\mathrm{Fe} + \left(\frac{3}{4}x + \frac{3fy}{2}\right)\mathrm{H_2O}. \quad [9]$$

Therefore, as reported in Table 3, upper and lower limits for the number of surface Fe atoms in the Pt–Fe clusters can be established by assuming that the corresponding Fe^{3+} atoms are reduced to either the ferrous or the zero-valent state, respectively. These calculations indicate that only a small fraction of Fe exists in bimetallic crystallites with Pt, except at low loadings of Fe. Increasing the Fe loading also decreases the concentration of surface Pt(Pt_s), which can be attributed to the coverage of Pt crystallites by Fe as the Pt/Fe ratio decreases.

Carbon as a support appears to significantly affect the behavior of the Pt–Fe particles regarding the H_2–O_2–H_2–O_2 titration sequence, as exhibited by the 0.6Pt–5Fe/carbon sample. The amount of reducible Fe estimated from this titration sequence was significantly higher than that in a SiO_2-supported Pt–Fe catalyst with similar metal loadings, which would suggest that there is a large fraction of Fe atoms in intimate contact with Pt in this Pt–Fe/carbon catalyst. In addition, the O_2 uptake in Step 4 of the titration sequence was higher than that needed to titrate the adsorbed hydrogen, chemisorb on Pt_s, and reoxidize the Fe surface. Further oxidation of Fe during Step 4 was unlikely because the catalyst should have been passivated during the first O_2 exposure in Step 2. One possible explanation for this increase in O_2 uptake is oxygen chemisorption on the carbon surface, which may be facilitated by the presence of water formed during titrations in the same manner as H_2 spillover can be assisted by water (31–33). This water can accumulate in the micropores and the metal–support interfacial region. Thus, it is conceivable that the number of surface Fe atoms in these carbon-supported Pt–Fe particles was overestimated because the likelihood of hydrogen spillover during the H_2 titration reaction in Step 3 is greater in this catalyst. Even in the absence of water, hydrogen spillover occurs more significantly on carbon than SiO_2 (32–35). The reason for the increase of O_2 uptake in Step 4, however, is still unknown because the influence of water on oxygen spillover has not been studied. In summary, the titration model developed here does not readily explain the H_2–O_2–H_2–O_2 titration behavior of carbon-supported Pt–Fe bimetallic particles.

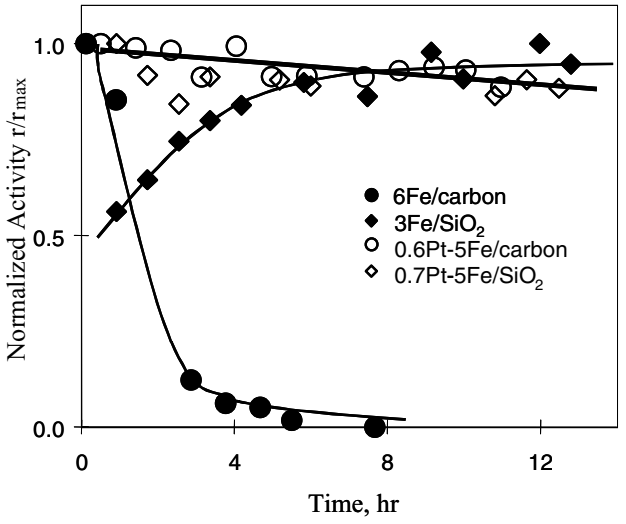

FIG. 2. Activity for acetic acid reduction versus time on stream for Fe and Pt–Fe catalysts supported on SiO_2 or carbon.

Catalytic Behavior

The effect of Pt addition to Fe catalysts can be readily seen by comparing the activity maintenance profiles for monometallic Fe and bimetallic Pt–Fe particles supported on either SiO_2 or carbon, as shown in Fig. 2. Under these reaction conditions, Pt alone exhibited no catalytic activity for acetic acid reduction to acetaldehyde and/or ethanol, and only decomposition to CH_4, CO, CO_2, and H_2O via decarbonylation and decarboxylation pathways was observed (1). Dramatic changes were observed in the activity profiles for both SiO_2-supported and carbon-supported Fe catalysts due to the addition of Pt. Before steady-state activity is achieved, an induction period of 4 to 5 h is typically observed for monometallic Fe catalysts (2), but it no longer occurs with these Pt–Fe catalysts. Instead, the activity of a bimetallic catalyst begins with a higher value before it declines somewhat to approach a steady-state activity. This behavior is markedly similar to that of a Pt/TiO_2 catalyst (1).

The Pt–Fe/C catalyst showed even greater contrasting behavior compared to its monometallic counterpart; i.e., severe deactivation, which was a major problem with Fe/C catalysts, did not occur after the addition of Pt. This deactivation has been attributed to the formation of an iron carbide (θ-Fe_3C) under reaction conditions, which inhibits sites important for the reaction and renders the surface of iron inactive (14). The presence of this carbide in a Fe/C

catalyst was previously detected by Mössbauer spectroscopy; however, the Mössbauer spectrum of 0.6Pt–5Fe/carbon obtained after being on stream for 8 h at 553 K failed to show the presence of the aforementioned carbide phase. In addition, the absence of carbide formation in the catalyst was coupled with an usually high concentration of CH_4 in the product stream. Based on these observations, Pt may have prevented the formation of iron carbide by maintaining a constant source of surface hydrogen atoms to hydrogenate any carbon atoms deposited on the iron surface.

Another indicator that bimetallic Pt–Fe systems can be excellent catalysts for acetic acid reduction by H_2 is reflected in their high selectivity for acetaldehyde, particularly at low Pt/Fe ratios. As shown in Fig. 3, which compares product selectivities among the SiO_2-supported Pt–Fe catalysts obtained near 10% conversion, the selectivity was strongly dependent on the relative amounts of Pt and Fe (Pt/Fe atomic ratios). Acetaldehyde was favored at very low Pt/Fe ratios and, as the amount of Pt increased, more ethanol was formed; then, at high Pt/Fe ratios a steady increase occurred in the formation of decomposition products—CH_4, CO, and CO_2. Ethanol formation began to decrease around Pt/Fe = 0.5, and eventually the product composition was dominated by CH_4, CO, and CO_2 at higher ratios. Except for a small amount of ethyl acetate (<3%), no other products were detected at this level of conversion (note that selectivity was calculated based only on the carbon-containing products).

Product selectivity was also influenced by acetic acid and hydrogen partial pressures, P_{HOAc} and P_{H_2}, respectively. Figure 4 shows that P_{HOAc} and P_{H_2} have opposite effects on the product selectivity over 0.7Pt–5Fe/SiO_2, which is represented as the mole ratio of acetaldehyde to ethanol, S_{ALD}/S_{ALC}, obtained at conversions below 10%. An increase in the acetic acid partial pressure increased S_{ALD}/S_{ALC}, whereas an increase in the hydrogen partial pressure decreased this ratio. Furthermore, these effects became more pronounced as the temperature increased, and it appears that selectivity to acetaldehyde, relative to ethanol, is enhanced at higher reaction temperatures.

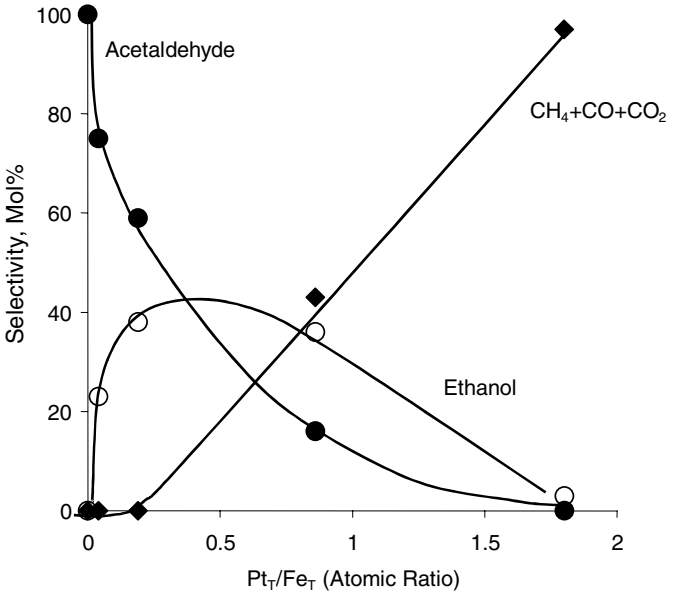

FIG. 3. Selectivity behavior demonstrated by a series of Pt–Fe/ SiO_2 catalysts with various atomic Pt/Fe ratios. Reaction conditions: H_2/HOAc= 47.6, WHSV = 19.7 L (STP) g^{-1} h^{-1}, P = 1 atm, Conv. = ~10%.

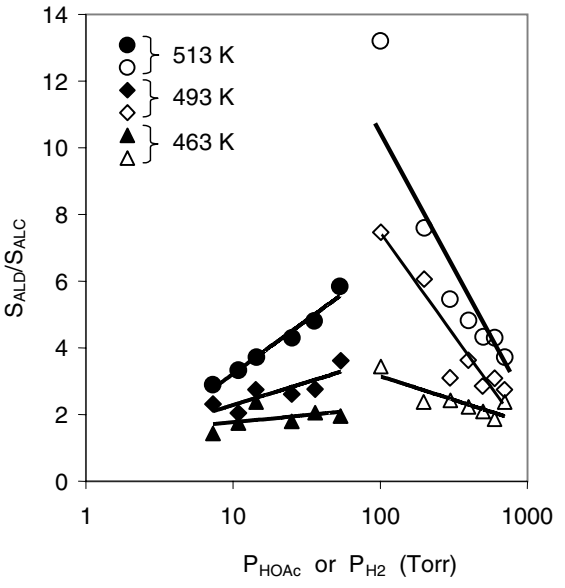

FIG. 4. Effects of acetic acid and hydrogen partial pressures (P_{HOAc} and P_{H_2}, respectively) on product selectivity (S_{ALD}/S_{ALC} = mole ratio of acetaldehyde and ethanol) of 0.7Pt–5Fe/SiO_2. Filled symbols are data obtained by varying P_{HOAc} and open symbols are those obtained by varying P_{H_2}. Conv. = ~10%.

One parameter that represents intrinsic kinetic behavior related to the combination of Pt and Fe is the apparent activation energy, E_a, that was measured for acetic acid reduction under standard reaction conditions. These values for Pt–Fe catalysts are consistently lower than that for a monometallic Fe catalyst, as shown in Table 4, with values

TABLE 4

Activity and Apparent Activation Energy for Acetic Acid Reduction on Pt–Fe Catalysts[a]

Catalysts	Hydrogenation activity (μmol HOAc/s/gcat)	E_a (kcal/mol)
0.7Pt–0.1Fe/SiO_2	0.012	16
0.7Pt–0.2Fe/SiO_2	0.28	13
0.7Pt–1Fe/SiO_2	1.75	15
0.7Pt–5Fe/SiO_2	2.21	14
3Fe/SiO_2	0.16	24
0.7Pt–5Fe/carbon	0.76	18
0.7Pt/TiO_2 (HTR)[b]	7.14	13

[a] T = 523 K, P_{HOAc} = 14 Torr, P_{H_2} = 700 Torr.
[b] Reference (1).

approaching those for Pt/TiO_2 catalysts, thus indicating that the addition of Pt may indeed alter the intrinsic kinetics of acetic acid hydrogenation over Fe catalysts. In addition, it was also observed that the minimum temperature at which the reaction can be detected is significantly lower for a Pt–Fe catalyst than that for an Fe-only catalyst; for example, $3Fe/SiO_2$ showed negligible activity below 473 K whereas all the Pt–Fe catalysts were active below 423 K. This significant enhancement in activity can undoubtedly be attributed to the addition of Pt, which is expected to actively engage in the catalytic cycle by providing sites for dissociatively adsorbing hydrogen. Again, this minimum temperature is also strikingly similar to that typically observed for a Pt/TiO_2 catalyst (1).

The fact that a Pt–Fe catalyst has a much higher activity for acetic acid reduction by H_2 than a monometallic Fe catalyst with a higher Fe loading indicates that the addition of Pt increases activity; however, before activity enhancement truly can be verified, comparison among these different catalyst systems must be made in terms of their specific activities. Thus, the rate data must be normalized to an appropriate basis in order to properly compare the activity performance of these monometallic Fe and bimetallic Pt–Fe catalysts. Previously, the reduction activity of monometallic Pt and Fe catalysts was normalized to the number of surface metal atoms determined by selective chemisorption to obtain a turnover frequency (TOF, molecule/s/M_s). The bimetallic catalyst systems, however, consist of surface Pt and Fe atoms that can exist in bimetallic as well as monometallic clusters dispersed on the supports, and this complexity presents some uncertainty in reporting their specific activity. The hypothesis that acetic acid reduction requires two types of sites—one set comprised of Pt (or Fe^0) atoms and the other set existing on the Fe oxide surface—further complicates a quantitative evaluation of this bimetallic system. Regardless, estimates can be made.

The total number of surface Pt atoms, Pt_s, and the number of surface Fe atoms that are in bimetallic crystallites, $Fe_{s,bi}$, can be estimated using the H_2–O_2–H_2–O_2 titration method described earlier; however, the number of surface Fe atoms that are not in bimetallic crystallites, which increases as Pt/Fe ratios become $\ll 1$, cannot be precisely determined. Nonetheless, as pointed out earlier, it is known that the specific activity associated with these monometallic Fe particles is very low (2); thus, little or no contribution to catalytic performance occurs at the lower temperatures used here and the measured activity is attributed only to the bimetallic clusters. The question then becomes how to normalize the activity with respect to Pt_s and $Fe_{s,bi}$. Figure 5 compares the TOF for acetic acid reduction with H_2 on $3Fe/SiO_2$, Pt/SiO_2, the series of $Pt–Fe/SiO_2$ catalysts, and $0.7Pt/TiO_2$. In this figure, the activity for $3Fe/SiO_2$ is normalized to Fe_s atoms, as determined by CO chemisorption at 195 K assuming a CO/Fe_s ratio of 0.5 (2), and that for

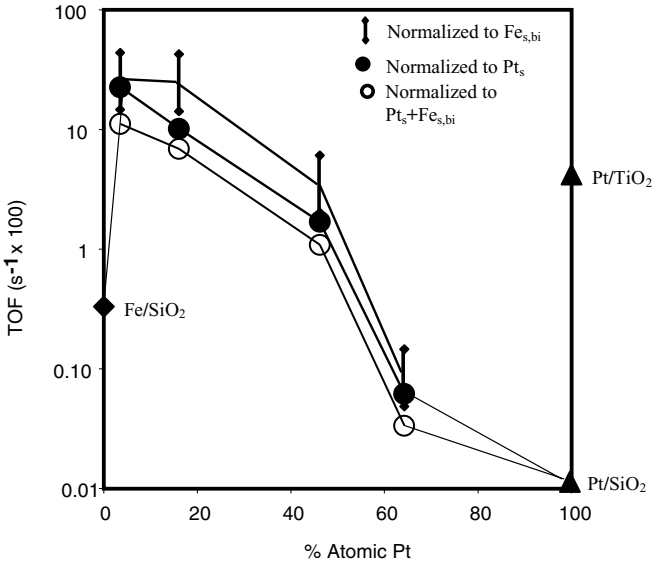

FIG. 5. Steady-state turnover frequency for acetic acid reduction over $Pt–Fe/SiO_2$ catalysts compared to Fe/SiO_2, Pt/SiO_2, and Pt/TiO_2. The range based on upper and lower estimates of $Fe_{s,bi}$ is indicated by an arrow. The uncertainty of other values is comparable to the symbol size. Reaction conditions: 523 K, 1 atm, $H_2/HOAc = 48$, conv. < 10%.

$0.7Pt/TiO_2$ is normalized to Pt_s atoms, as determined by H_2 chemisorption, whereas activities for the $Pt–Fe/SiO_2$ catalysts are represented by TOFs based on Pt_s, on the surface bimetallic Fe atoms ($Fe_{s,bi}$), or on the sum of Pt_s and $Fe_{s,bi}$. In the last calculation, the median value of $Fe_{s,bi}$ is used. The TOF calculated based on $Fe_{s,bi}$ is represented as a range of values (shown by vertical bars) because the number of surface Fe atoms in the bimetallic clusters was estimated using both the upper and the lower limits determined in Table 3. Regardless of the choice, an enhancement in TOF relative only to Fe is clearly seen with all of the $Pt–Fe/SiO_2$ catalysts except $0.7Pt–0.1Fe/SiO_2$, and all TOF values for reduction are higher than that on Pt/SiO_2, which exhibited primarily decomposition activity (1, 11). Catalysts with low Pt/Fe ratios, i.e., $0.7Pt–1.0Fe/SiO_2$ and $0.7Pt–5Fe/SiO_2$, show a TOF that is one to two orders of magnitude higher than that on monometallic Fe/SiO_2 and is even higher than that on TiO_2-supported Pt, which is a very active catalyst for acetic acid reduction with H_2.

Reaction Mechanism

The kinetic behavior of these Pt–Fe systems has many similarities to that of TiO_2-supported Pt, as evidenced by a comparison of specific activities, apparent activation energies, and activity maintenance behavior. Acetic acid reduction over monometallic Fe/SiO_2 and Pt/TiO_2 catalysts has been proposed to proceed via a dual-site mechanism, but with different principal active surface intermediates on each catalyst (1, 2, 11). The addition of Pt to Fe catalysts

indicates that Pt–Fe crystallites give rise to kinetic behavior that differs from that usually observed with monometallic Fe catalysts.

In the general scheme of acetic acid reduction by H_2 over Pt/TiO_2 and Fe/SiO_2 catalysts, acetaldehyde and ethanol are formed by sequential reactions, i.e., acetic acid is first reduced to acetaldehyde, which may or may not desorb, and is then further hydrogenated to ethanol (1, 2). The influences of acetic acid and hydrogen partial pressures as well as temperature on selectivity, as shown in Fig. 4, imply that the same scheme can be applied to these Pt–Fe catalysts. For example, increasing the acetic acid partial pressure increased acetaldehyde selectivity because the surface coverage of acetaldehyde decreased due to greater competition by acetic acid for active sites. Conversely, a higher hydrogen partial pressure resulted in higher hydrogen surface coverages and thus favors more complete hydrogenation to ethanol. The effect of temperature on selectivity will depend on the relative heats of adsorption of the various reactants as well as activation energies for the various reactions. Increasing the Pt/Fe ratio favored ethanol formation, which is consistent with the proposed reaction mechanism because an increase in Pt_s in the catalyst would increase in the surface concentration of hydrogen atoms.

To further investigate the role of Pt–Fe crystallites in acetic acid reduction, other than providing sites that facilitate H_2 dissociation, surface species were examined using DRIFTS, and Fig. 6 displays spectra of surface species detected following acetic acid adsorption on $0.7Pt–5Fe/SiO_2$, $3Fe/SiO_2$, and $0.7Pt/SiO_2$ at 300 K. A new infrared band at 1690 cm^{-1} can be clearly seen on the Pt–Fe catalyst and, because this band was not detected on either Pt/SiO_2 or Fe/SiO_2, this band is assigned to a surface species on sites existing only on bimetallic Pt–Fe surfaces. The IR bands at 1748 cm^{-1} and 1725 cm^{-1} are attributed to the carbonyl stretching mode, $\nu(C{=}O)$, of surface silyl ester groups and hydrogen-bonded molecular acetic acid adsorbed on the SiO_2, respectively, and those at 1581 and 1454 cm^{-1} are assigned to the $\nu_a(COO)$ and $\nu_s(COO)$ frequencies of surface acetate species (36). The latter species can form on either Pt or Fe surfaces. The new band at 1690 cm^{-1} is similar to an IR band at 1680 cm^{-1}, observed following acetic acid adsorption on Pt/TiO_2, which was assigned to a surface acyl species

$$(CH_3\,\overset{\overset{O}{\|}}{C}\,{-}*),$$

and it has been proposed that this surface acyl species is an active intermediate during acetic acid reduction on this catalyst (11). Although surface acetate may also be an active intermediate, as proposed for monometallic Fe catalysts (2, 13), acyl species are more reactive and more susceptible to hydrogenation at lower temperatures, as evidenced by TPR experiments (37). The presence of this species is concurrent with a higher activity and a lower apparent activation energy, similar to those of a Pt/TiO_2 catalyst; consequently, the band at 1690 cm^{-1} is attributed to the carbonyl stretch mode of an acyl surface species on the surface of bimetallic Pt–Fe particles. By drawing another analogy to Pt/TiO_2, the sites at which this acyl species are formed are proposed to exist on an oxidic Fe surface. The Mössbauer spectrum of $0.7Pt–5Fe/SiO_2$ obtained after it was subjected to reaction conditions shows the presence of Fe^{2+}, as shown in Fig. 7, so these acyl species are presumed to form on FeO phases in the Pt–Fe particles. The spectral parameters are listed in Table 5.

Although both acyl and acetate species are present on the catalyst surface and both may be active intermediates during acetic acid reduction to acetaldehyde, the reduction pathway involving the former is more direct and has a lower energy barrier because it requires only the addition of a hydrogen atom to a very reactive acyl species to form acetaldehyde. Thus, the reaction mechanism on a $Pt–Fe/SiO_2$ catalyst is proposed to be essentially the same as that proposed for Pt/TiO_2 catalysts and, to substantiate this proposal, the rate data obtained at various acetic acid and H_2 partial pressures were fitted to the same kinetic model used to describe the reaction over TiO_2-supported Pt. This reaction sequence is a Langmuir–Hinshelwood-type model invoking two types of sites, one set on Pt, designated as $*$ sites, where both hydrogen and acetic acid dissociatively adsorb to produce surface hydrogen atoms and a surface acetate species, and the other set involving FeO, designated as *S* sites, on which acetic acid molecularly adsorbs and

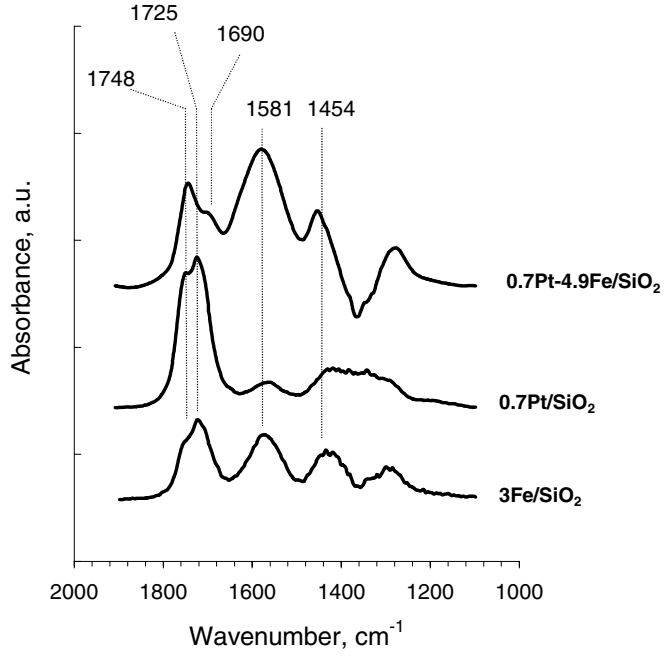

FIG. 6. DRIFT spectra of surface species after acetic acid adsorption at 300 K on $3Fe/SiO_2$, $0.7Pt/SiO_2$, and $0.7Pt–5Fe/SiO_2$.

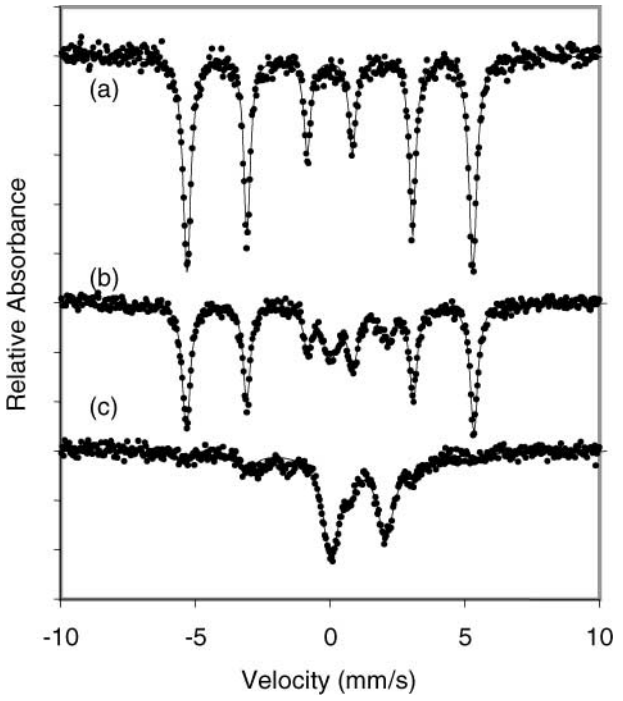

FIG. 7. Mössbauer spectra of 0.7Pt–5Fe/SiO_2 at 300 K: (a) after reduction at 723 K; (b) and (c) after 8 min and 8 h on stream at 553 K, respectively. Spectral parameters are listed in Table 5.

dissociates to form surface acyl species. The rate expression is derived based on the sequence of elementary steps depicted below (11).

$$H_{2(g)} + 2^* \overset{K_{H_2}}{\rightleftharpoons} 2H^* \quad [10]$$

$$CH_3COOH_{(g)} + 2^* \overset{K_{Ac}}{\rightleftharpoons} CH_3COO^* + H^* \quad [11]$$

$$CH_3COOH_{(g)} + S \overset{K_A}{\rightleftharpoons} CH_3COOH\text{–}S \quad [12]$$

$$CH_3COOH\text{–}S \overset{K_{Acy}}{\rightleftharpoons} CH_3CO\text{–}S\text{–}OH \quad [13]$$

$$CH_3CO\text{–}S\text{–}OH + H^* \xrightarrow{k_1} CH_3COH\text{–}S\text{–}OH + ^* \quad [14]$$

$$CH_3COH\text{–}S\text{–}OH + H^* \xrightarrow{k_2} CH_3CHO\text{–}S + + {}^*H_2O_{(g)} \quad [15]$$

$$CH_3CHO\text{–}S \underset{k_{-3}}{\overset{k_3}{\rightleftharpoons}} CH_3CHO_{(g)} + S \quad [16]$$

$$CH_3CHO\text{–}S + H^* \xrightarrow{k_4} CH_3CHOH\text{–}S + ^* \quad [17]$$

$$CH_3CHOH\text{–}S + H^* \xrightarrow{k_5} CH_3CH_2OH\text{–}S + ^* \quad [18]$$

$$CH_3CH_2OH\text{–}S \underset{k_{-6}}{\overset{k_6}{\rightleftharpoons}} CH_3CH_2OH_{(g)} + S \quad [19]$$

Based on this sequence of elementary steps and assuming that H atoms and acetate species dominate on the $*$ sites while molecular acetic acid and acyl species are the most abundant surface intermediates on the S sites, the rate of acetic acid reduction by H_2, $r_{HOAc} = \frac{-d[HOAc]}{dt}$, is:

TABLE 5

Mössbauer Spectral Parameters for 0.7Pt–5Fe/SiO_2[a]

Conditions	Phase	IS (mm/s)	QS (mm/s)	HF (kOe)	SC (%)
After reduction at 723 K for 1 h	α-Fe	0.0	0.0	331	100
After 8-min reaction at 553 K	α-Fe	0.0	0.0	332	73
	Fe^{2+}	1.08	2.08	—	16
	Fe^{3+}	0.44	0.89	—	11
After 8-h reaction at 553 K	α-Fe	0.0	0.0	337	23
	Fe^{2+}	1.06	2.00	—	65
	Fe^{3+}	0.36	0.75	—	12

[a] After being subjected to conditions shown in Fig. 7. IS, isomer shift; QS, quadrupole splitting; HF, hyperfine field; and SC, spectral contribution.

$$r_{HOAc} = \frac{k_1 K_{Acy} K_A K_{H_2}^{1/2} P_A P_{H_2}^{1/2}}{\left(K_{H_2}^{1/2} P_{H_2}^{1/2} + K_{Ac} P_A / K_{H_2}^{1/2} P_{H_2}^{1/2}\right)(1 + K_A(1 + K_{Acy}) P_A)}. \quad [20]$$

A complete derivation of this rate equation has been provided elsewhere (11). This rate equation was fitted to the reactant partial pressure rate data obtained with 0.7Pt–5Fe/SiO_2 using a least-squares nonlinear optimization method, and the results are shown in Fig. 8. The enthalpies

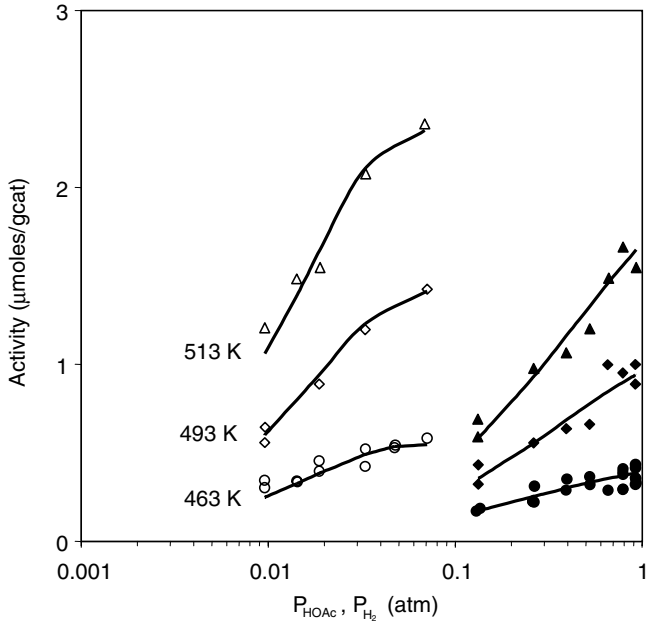

FIG. 8. Reduction activity of 0.7Pt–5Fe/SiO_2 obtained at various acetic acid and hydrogen partial pressures. Solid lines denote the optimum fits obtained by fitting Eq. [20] to the experimental data points. Empty symbols are activity data obtained at constant P_{H_2} and filled symbols are those obtained at constant P_{HOAc}.

TABLE 6

Enthalpies and Entropies of Adsorption from Rate Parameters[a]

Process	0.7Pt–5Fe/SiO_2		0.7Pt/TiO_2 (HTR)[b]	
	ΔH^0_{ad} (kcal/mol)	ΔS^0_{ad} (cal/mol/K)	ΔH^0_{ad} (kcal/mol)	ΔS^0_{ad} (cal/mol/K)
Dissociative H_2 ads. on Pt	−27	−28	−29	−38
Dissociative HOAc ads. on Pt	−22	−12	−20	−10
Dissociative HOAc ads. on FeO	−6[c]	−8[c]	−10[c]	−18[c]

[a] Standard state, 1 atm.
[b] From Ref. (11).
[c] Assuming acyl species are dominant on oxide sites.

and entropies of hydrogen and acetic acid adsorption obtained from the temperature dependence of the equilibrium adsorption constants, K_{H_2} and K_{Ac}, are reported in Table 6. The reaction model correlates the experimental data very satisfactorily, and the enthalpy and entropy of adsorption for acetic acid and hydrogen on Pt obtained from the fitted parameters are thermodynamically consistent, with the entropy of adsorption satisfying additional constraints and guidelines (38, 39). These values are very similar to those obtained for a Pt/TiO_2 catalyst (see Table 6). Furthermore, the enthalpy and entropy for dissociative adsorption of acetic acid on the oxide sites to form an acyl species are similar to values reported earlier for titania. The results of this kinetic modeling are consistent with the conclusion that the addition of Pt to an Fe catalyst can alter the reaction pathway from one involving surface acetate species to one having acyl surface species as the principal active intermediate.

SUMMARY

Supported Pt–Fe catalysts were characterized by successive H_2–O_2–H_2–O_2 titration cycles conducted at 300 K as well as by Mössbauer spectroscopy and DRIFTS. The formation of bimetallic Pt–Fe crystallites in these catalysts was verified by the reversible oxidation–reduction of iron observed during this titration sequence. A model was proposed which described these titration results and allowed an estimation of the number of surface Pt and Fe atoms in the bimetallic particles dispersed on SiO_2. The H_2–O_2–H_2–O_2 titration sequence with a carbon-supported Pt–Fe catalyst was different, however, and it deviated from this model. This behavior was attributed to hydrogen spillover coupled with irreversible oxygen adsorption on the carbon surface.

The addition of Pt to Fe to form bimetallic Pt–Fe particles increased the reducibility of iron during the reduction pretreatment, enhanced activity, eliminated the induction period, lowered the apparent activation energy, and yet maintained a high selectivity to acetaldehyde, particularly with catalysts with low Pt/Fe ratios. The severe deactivation that occurred with Fe/carbon catalysts, which has been associated with the formation of iron carbide, was also prevented by the addition of Pt.

It is proposed that acetic acid reduction with H_2 over bimetallic Pt–Fe catalysts occurs via a rate-determining surface reaction between a hydrogen atom and surface acyl species, and the kinetics can be described by a rate expression derived from a Langmuir–Hinshelwood-type model invoking hydrogen dissociation on Pt sites and acetic acid adsorption and activation on an FeO phase to create the surface acyl species.

ACKNOWLEDGMENT

This study was sponsored by the DOE, Division of Basic Energy Sciences, via Grant DE-FG02-84ER13276.

REFERENCES

1. Rachmady, W., and Vannice, M. A., *J. Catal.* **192**, 322 (2000).
2. Rachmady, W., and Vannice, M. A., *J. Catal.*, in press.
3. Vannice, M. A., and Garten, R. L., *J. Mol. Catal.* **1**, 201 (1975/76).
4. Guczi, L., *Catal. Lett.* **7**, 205 (1990), and references therein.
5. Woo, H. S., Fleisch, T. H., Foley, H. C., Uchiyama, S., and Delgass, W. N., *Catal. Lett.* **4**, 93 (1990).
6. Sakamoto, Y., Higuchi, K., Takahashi, N., Yokota, K., Doi, H., and Sugiura, M., *Appl. Cat. B* **23**, 159 (1999).
7. Kim, K. T., Hwang, J. T., Kim, Y. G., and Chung, J. S., *J. Electrochem. Soc.* **140**, 31 (1993).
8. Hwang, J. T., and Chung, J. S., *Electrochim. Acta* **38**, 2715 (1993).
9. Wan, C. Z., Eur. Patent 129,399 (1984).
10. Bartholomew, C. H., and Boudart, M., *J. Catal.* **29**, 278 (1973).
11. Rachmady, W., and Vannice, M. A., *J. Catal.* **207**, 317 (2002).
12. Benesis, H. A., Curtis, R. M., and Studer, H. P., *J. Catal.* **10**, 328 (1968).
13. Chen, A., Kaminsky, M., Geoffroy, G. L., and Vannice, M. A., *J. Phys. Chem*. **90**, 4810 (1986).
14. Rachmady, W., and Vannice, M. A., *J. Catal.*, in press.
15. Benson, J. E., and Boudart, M., *J. Catal.* **4**, 704 (1965).
16. Freel, J., *J. Catal.* **25**, 139 (1972).
17. Garten, R. L., *J. Catal.* **43**, 18 (1976).
18. Kruger, J., and Yolken, H. T., *Corros. Abstr.* **20**, 29 (1964).
19. Menon, P. G., and Skaugset, P., *Appl. Catal. A* **115**, 295 (1994).
20. Baranski, A., Pattek, A., and Reizer, A., *Bull. Acad. Polonaise Sci. Ser. Sci. Chim.* **26**, 353 (1978).
21. Topsøe, H., Dumesic, J. A., and Boudart, M., *J. Catal.* **28**, 477 (1973).
22. Tsarev, V. I., Aptekar, E. L., Krylova, A. V., and Torocheshnikov, T. S., *React. Kinet. Catal. Lett.* **14**, 279 (1980).
23. Bartholomew, C. H., Anderson, J. H., and Boudart, M., *J. Chem. Soc. Faraday Trans. 1* **75**, 257 (1979).
24. Wilson, G. R., and Hall, W. K., *J. Catal.* **17**, 190 (1970).
25. Benson, J. E., and Boudart, M., *J. Catal.* **4**, 704 (1965).
26. Freel, J., *J. Catal.* **25**, 139 (1972).
27. Wilson, G. R., and Hall, W. K., *J. Catal.* **24**, 306 (1972).

28. Vannice, M. A., Benson, J. E., and Boudart, M., *J. Catal.* **16**, 348 (1970).
29. Palmer, M., and Vannice, M. A., *J. Chem. Technol. Biotechnol.* **30**, 205 (1980).
30. Dézsi, I., Nagy, D. L., Eszterle, M., and Guczi, L., *React. Kinet. Catal. Lett.* **8**, 301 (1978).
31. Levy, R. B., and Boudart, M., *J. Catal.* **32**, 304 (1974).
32. Teichner, S. J., *Stud. Surf. Sci. Catal.* **77**, 27 (1993).
33. Boudart, M., Vannice, M. A., and Benson, J. E., *Z. Phys. Chem. N.F.* **64**, 171 (1969).
34. Conner, W. C., Pajonk, G. M., and Teichner, S. J., *Adv. Catal.* **34**, 1 (1986).
35. Lenz, D. H., and Conner, W. C., *J. Catal.* **112**, 116 (1988).
36. Nakamoto, K., "*Infrared and Raman Spectra of Inorganic and Coordination Compounds*," 4th ed. Wiley, New York, 1986.
37. Rachmady, W., Ph.D. thesis. The Pennsylvania State University, University Park, 2001.
38. Boudart, M., *AIChE J.* **18**, 465 (1972).
39. Vannice, M. A., Hyun, S. H., Kalpacki, B., and Liauh, W. C., *J. Catal.* **56**, 358 (1979).